3D-printed Electrodes for Sensing of Biologically Active Molecules

*Bella Rosa Liyarita, Adriano Ambrosi, Martin Pumera**

Division of Chemistry & Biological Chemistry, School of Physical Mathematical Science, Nanyang Technological University, Singapore 637371, Singapore

*Email: pumera.research@gmail.com

Abstract

3D printing (additive manufacturing) is currently an emerging technology that could revolutionize the traditional manufacturing process. The application of 3D printing technology has been examined in many different fields including manufacturing, science, medicine, and electronics. Another application of 3D printing technology which holds promising potential is fabrication of electrochemical sensors and transducers. Electroanalytical devices hold advantages such as low cost, portability, ease of use, and rapid analysis. Here we examined the feasibility of utilizing 3D-printed metal electrodes for the electrochemical detection of the pain reliever acetaminophen (AC) also known as paracetamol and the neurotransmitter dopamine (DA) in aqueous solutions. 3D-printed stainless steel helical-shaped electrodes were tested before and after surface modification by electro-plating with a thin gold film (3D gold).

KEYWORDS: Additive manufacturing, electrochemistry, electroplating, gold electrode, pharmaceutical.

Introduction

3D printing technology, also known as additive manufacturing is a process of making a three-dimensional object from a digital file by adding a successive layer of materials until the desired object is created.[1] 3D printing is now an emerging technology which holds great potentials to transform conventional centralized manufacturing processes to a futuristic concept where end users are able to design and produce on their own using cheaper and simpler printing machines.

Currently, it is possible to 3D print objects of any size and complex structure using a wide range of materials such as thermoplastics, metals, ceramics, and even living cells.[2,3,4] Numerous researches and developments for 3D printing have been growing in the past decade and its application in different fields have been examined. Some applications are found in the area of manufacturing, engineering, tissue and organ fabrication, and orthopedic implants.[5,6] Another application that can benefit from 3D printing technology is the development of novel electroanalytical devices and systems.[7] Electrochemical sensing and analytical devices are widely used in diverse industries as they provide advantages such as low cost, ease of use, portability, and rapid analysis[8,9] over conventional analytical instrumentation. 3D printing technology can be utilized, for example, to fabricate with high precision and uniformity the electrochemical transducer (electrode) of the sensing device using conductive materials.[10] Electrodes of any shapes and materials can be created in a few hours by a simple process at reduced cost with benefits for rapid prototyping.

Acetaminophen (N-acetyl-p-aminophenol or Paracetamol, AC) is an antipyretic and analgesic drug which is widely used for mild to moderate pain reliever and fever reducer.[11,12,13] It is non-carcinogenic and an effective alternative for patients who are sensitive to aspirin. AC is sometimes used for cancer pain management and osteoarthritis therapy. It is rapidly absorbed and distributed after oral administration and is metabolized predominantly in the liver to generate toxic metabolites. Generally, AC is considered safe when administered up to therapeutic doses, however, overdoses in few cases may lead to accumulation of some liver and nephrotoxic metabolites and eventually causing hepatotoxicity, nephrotoxicity, and renal failure. As paracetamol drug is increasingly used for therapeutic uses, fast and accurate determination of AC is highly needed.

Dopamine (3,4-dihydroxyphenetylamine, DA) is one of the main neurotransmitters of the catecholamine group which plays a significant role in our central and peripheral nervous system.[12,14] It also plays an important role in human metabolism, cardiovascular, renal, and hormonal system. The deficiency or sufficiency of DA induces neurological disorders such as Schizophrenia, Huntington's disease, Parkinson's disease, and restless leg syndrome (RLS) by deregulating its concentration in brain and blood.[12,14,15,16] DA metabolites leave the body through urine and the measurement of the catecholamine level in the body can be done by the urine test.[17,18,19] The test is also done to look for signs of pheochromocytoma, which is a type of tumor that grows on adrenal glands and produces excess catecholamine.[19]

An important drug such as AC will interfere the measurement of catecholamine in the biological sample. AC interacts with DA to decrease the concentration level of DA metabolites and may induce neurological diseases.[15,16] Therefore, it is important to measure the concentration of AC in presence of DA and resolve the two competing electrochemical signals to test the sensitivity of the electrode to determine the concentration of each analyte.

Voltammetric techniques such as cyclic voltammetry (CV) and differential pulse voltammetry (DPV) were used to assess the performance of a helical shaped stainless steel 3D-printed electrode for the detection of acetaminophen and dopamine. The electrode was fabricated using selective laser melting (SLM) method, in which a high-power laser fully melts and binds each layer from a metal powder bed. Furthermore, the 3D-printed stainless steel electrode was surface-modified with a thin gold layer by electro-plating to improve the electrochemical performance. The gold-plated and as-produced 3D-printed stainless steel electrodes were tested in comparison to conventional glassy carbon and gold disk electrodes.

EXPERIMENTAL SECTION

Materials. Potassium phosphate monobasic, sodium phosphate dibasic, potassium chloride, sodium chloride, potassium hydroxide, acetaminophen, and dopamine hydrochloride were purchased from Sigma Aldrich, Singapore. Hydrogen peroxide (35%, w/w) was purchased from

Alfa Aesar, Singapore. Milli-Q water with a resistivity of 18.2 MΩ cm was used throughout the experiment.

Apparatus. Scanning electron microscopy (SEM) was conducted with a JEOL JSM-7600F semi-in-lens field-emission scanning electron microscope. The energy dispersive X-ray spectroscopy (EDX) data were obtained with an Oxford instrument and analyzed by using Aztec software. All voltammetry measurements were performed at room temperature by using a three-electrode configuration on a Autolab type III electrochemical analyzer (Methrom Autolab B.V., The Netherlands) connected to a personal computer. The analyzer was controlled by NOVA software, version 1.10 (Methrom Autolab B.V.). A platinum electrode was employed as an auxiliary electrode, and an Ag/AgCl electrode was used as a reference electrode. Gold-plated 3D-printed electrode (18 mm^2 surface area), glassy carbon electrode (3mm diameter), and gold disk electrode (3mm diameter) were used as working electrodes. All electrochemical potentials in this report are quoted versus the Ag/AgCl reference electrode.

Fabrication of Helical-Shaped 3D-Printed Stainless Steel Electrodes. 3D-printed steel electrodes were obtained using a ConceptLaser printer (Concept Laser GmbH, Germany) which uses a selective laser melting (SLM) technique, as described in a previous work.[20] Briefly the electrode design was first drawn using sketch-up 3D modeling open-source software. A focused, high-energy laser beam fuses and link metallic particle deposited in powder form on a printing stage according to the established design in a layer by layer fashion. Stainless steel particles (CL 20ES, Concept Laser, GmbH) were employed to produce helical-shaped stainless steel electrodes.

Au electroplating of the 3D-printed Stainless Steel electrodes. Au electroplated electrodes were obtained as previously reported.[10] Briefly, the 3D printed stainless steel electrode was immersed into a commercial gold plating solution and the deposition was carried out by applying a current of -20 mA for 90 min while stirring in the presence of a Ag/AgCl reference electrode and a platinum auxiliary electrode.

Electrochemical Measurement. A stock solution of 5 mM AC and 5 mM DA were prepared separately. A calculated amount of the stock solution was added to 7mL phosphate buffer solution (pH 7.2) to obtain the desired concentration of the solution in the electrochemical cell. Standard addition method was employed to increase the concentration of the solution in the electrochemical cell. Prior to the start of the measurement, the gold-plated 3D-printed electrode was cleaned by soaking the electrode in a mixture of H_2O_2 (25% v/v) and KOH (50 mM) for 10 minutes to dissolve and desorb contaminants then followed by cyclic voltammetry from -1 V to 0 V in 50 mM KOH.[21] The glassy carbon and gold disk electrodes were polished with alumina powder (0.05 mm) on a polishing pad before every measurement. All measurements were carried out in phosphate buffer solution (pH 7.2) at a scan rate of 0.1 V s^{-1}.

Determination of Acetaminophen in Pharmaceutical Tablet. The gold-plated 3D-printed sensor was tested for the determination of AC on the pharmaceutical tablets. Panadol® (GSK, Singapore) tablets containing 500mg were used for the measurement. The tablets were weighed, ground into powder, and then dissolved in ultrapure water. The solution was then diluted and filtered using 0.2µm Supor® Membrane (PALL Life Science) to obtain 10mM stock solution. The recovery tests were carried out in phosphate buffer solution (pH 7.2) using DPV technique for the determination of AC in pharmaceutical tablets.

RESULTS AND DISCUSSION

The electrode fabrication process starts with the electrode design obtained by means of a CAD software which is used by the 3D printer to produce a series of stainless steel electrodes (step I in Figure 1A). The steel electrodes are successively modified by Au electroplating to modify their surface (step II in Figure 1A). Surface modification upon Au electrodeposition can be easily noticed by the formation of a golden surface. Energy dispersive X-ray (EDX) and scanning electron microscopy (SEM) was employed to study the morphology and chemical composition of the electrode and to validate the success of electro-plating. Figure 1B-J shows the SEM image of a section of the bare stainless steel electrode before and after electro-plating with Au with the corresponding element mapping and EDX spectra. The presence of iron (Fe) and nickel (Ni) were dominant in the bare 3D-printed stainless steel electrode as the main components of steel.

After electro-plating, a distinctive Au signal was observed in the EDX spectrum (Figure 1J). Moreover, from the element mapping, the intensity of Fe and Ni was significantly decreased and Au resulted prominent (Figure 1H).

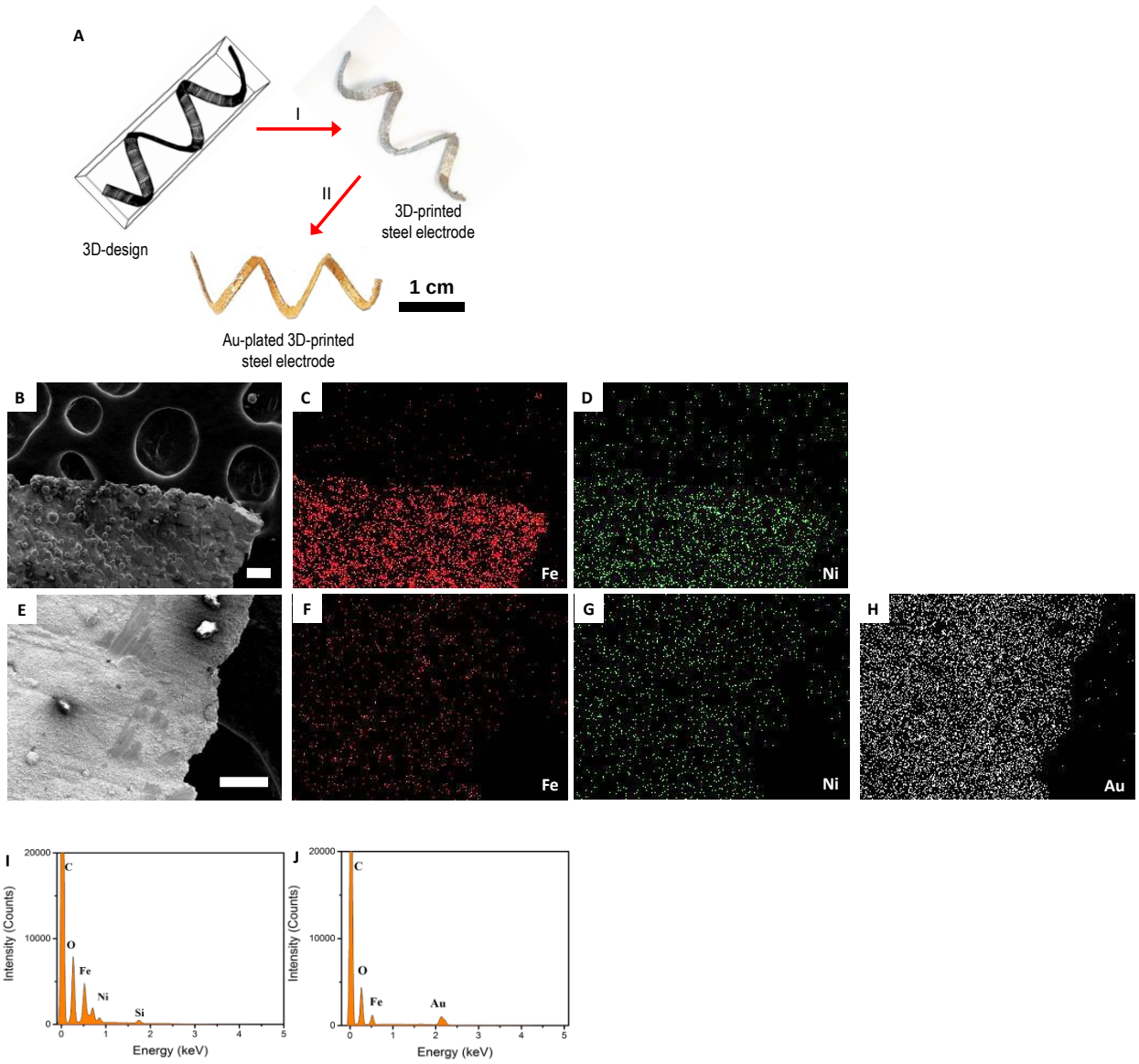

Figure 1. A) Schematic of the metal 3D-printed electrode fabrication and modification. The 3D virtual design has been used in step (I) to fabricate stainless steel electrodes by SLM 3D-printing technology. The steel electrode as-printed is then modified by Au electroplating in step (II). B) SEM image of a section of the bare 3D-printed stainless steel electrode and the corresponding element mapping of C) Fe and D) Ni. E) SEM image of a section of the Au-plated 3D-printed steel electrode and the corresponding element mapping of F) Fe, G) Ni and H) Au. I) EDX spectrum for the bare stainless steel electrode. J) EDX spectrum for the Au-plated 3D-printed steel electrode. Scale bar corresponds to 100 μm.

Electrochemical Behavior of Acetaminophen

The 3D-printed stainless steel electrode was first tested for the detection of acetaminophen (AC). The cyclic voltammetry (CV) and differential pulse voltammetry (DPV) measurements were carried out in 0.1 M phosphate buffer solution (pH 7.2). The concentration of AC was increased from 0.1 mM to 1 mM to determine the peak potential of AC and investigate the dependence of peak current and concentration. Acetaminophen undergoes a two-electron oxidation to form N-acetyl-p-benzoquinone (NAPQI) which can cause an adverse effect if the accumulation of NAPQI is high. The 3D-printed steel electrode produced undistinguished signal in the absence or presence of AC, therefore not adequate for this application. In contrast, the gold-plated 3D-printed (3D gold) electrode demonstrated enhanced sensitivity in detecting AC when compared to the commercial gold disk and glassy carbon (GC) electrodes (Figure 2). The electrochemical behavior of AC at the gold-plated 3D-printed (3D gold) electrode was evaluated using CV and DPV techniques, taking into consideration the different geometrical surface area. It can be seen in Figure 2A that a pair of redox peaks was observed using the three electrodes due to oxidation and reduction of AC at the electrode surface. At the 3D gold electrode, the anodic peak and cathodic peak were observed at about +0.40 V and +0.24 V respectively. Interestingly, more positive anodic peak at +0.47 V and cathodic peak at +0.10 V were observed at the gold disk electrode. Whereas, anodic peak at +0.42 V and cathodic peak at +0.17 V were observed at the GC electrode. It can be also noticed that the oxidation peak current density on the 3D gold electrode was enhanced by 4 and 7 folds in comparison to GC and gold disk electrode, respectively.

Peak to peak separation (ΔE_p) values corresponds to the potential difference of anodic and cathodic peak potential (E_{pa} - E_{pc}). Smaller ΔE_p value indicates faster electron transfer of AC at the electrode surface. The ΔE_p values were 156 mV for 3D gold, 251 mV for GC, and 373 mV for gold disk electrode. Clearly 3D gold showed the fastest electron transfer among the electrodes investigated. The DPVs more easily highlight the different oxidation potential of AC on the three electrodes as illustrated in Figure 2B. It is shown that the 3D gold electrode has the lowest peak potential at +0.34 V followed by GC at +0.37 V, and gold disk electrode at +0.44 V.

The decrease in peak potential, smaller ΔE_p value, and higher oxidation current density indicates that the 3D gold electrode demonstrates excellent electro-catalytic ability towards AC. A scan rate study was performed for the oxidation and reduction of AC on 3D gold electrode which demonstrated a diffusion-controlled process (See Figure S1 of Supporting Information).

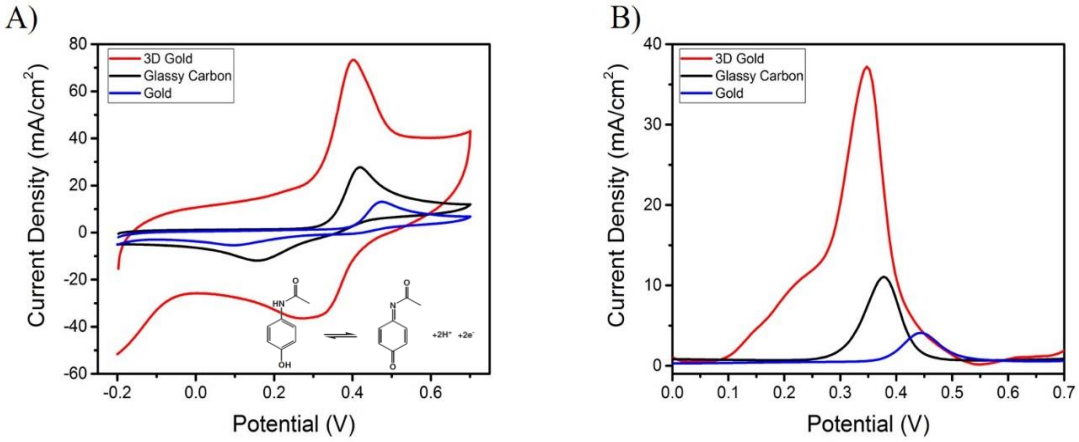

Figure 2. A) Cyclic voltammograms and B) Differential pulse voltammograms of 0.5 mM AC in 0.1 M phosphate buffer solution (pH 7.2) at the 3D gold, glassy carbon, and gold disk electrode.

Determination of Acetaminophen

The voltammetric quantification was carried out by CV and DPV techniques in 0.1 M phosphate buffer solution (pH 7.2) with increasing concentration of AC from 0.1 mM to 1 mM. The cyclic voltammograms of AC at the three electrodes are presented in Figure S2A-C. As observed, the oxidation and reduction peak currents increase proportionally as concentration increases. For all three electrodes, the anodic peak shifted towards positive potential while the anodic peak shifted towards negative potential. However, the potential shift was observed to be larger at the 3D gold electrode. Moving on, DPV was used to study the correlation of the concentration and peak current as it offers better sensitivity compared to CV. The study was conducted on the same concentration range of AC. Similar to the CV results, the current response resulted linearly proportional with the increase of AC concentration (Figure S2D-F). From the DPV results in Figure S2D-F, the peak current density was plotted against the concentration of AC to compare the sensitivity between the three electrodes. The plot is presented in Figure 3. A good linearity

was observed for all three electrodes which however differed in sensitivity as indicated by the slop value of the three plots. 3D gold electrode presented a slope of 33.03 mA cm^{-2} Mm^{-1} which resulted the highest if compared with the values of 18.66 mA cm^{-2} Mm^{-1} for the GC electrode and 7.01 mA cm^{-2} Mm^{-1} for the gold disk electrode. The sensitivity for AC detection at the 3D gold electrode is enhanced by about 1.8 times with respect to GC and 4.8 times with respect to the gold disk electrode.

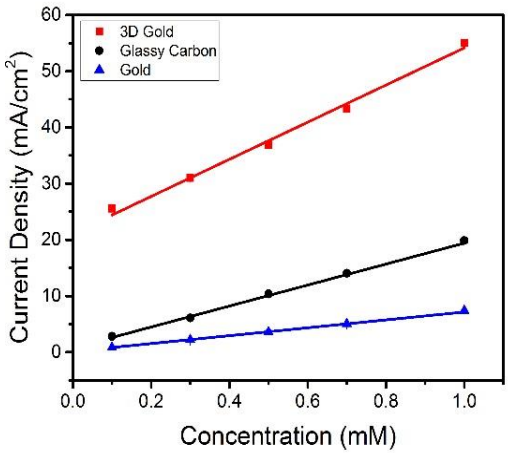

Figure 3. Calibration curve of the peak current density against the concentration of AC in the 0.1 M phosphate buffer solution (pH 7.2) at the 3D gold, glassy carbon, and gold disk electrode.

Electrochemical Behavior of Dopamine

Dopamine (DA) is an electroactive species and the redox reaction involves two electrons transfer to form dopamine *o*-quinone. CV and DPV measurements were conducted at gold-plated 3D-printed, glassy carbon and gold disk electrodes to study the electrochemical behavior of DA. The CVs in the presence of 150µM DA at the 3D gold, GC and gold disk electrode are presented in Figure 4A. Similar to AC, the CVs were conducted between -0.2 V – 0.7 V and a pair of well-defined DA redox peaks were observed using all three electrodes. The anodic peak at +0.17 V and cathodic peak at +0.11 V were observed at the 3D gold electrode and also gold disk electrode. Meanwhile, the GC electrode gave a more positive anodic peak at +0.21 V and more negative cathodic peak at +0.09 V. Moreover, the oxidation current peak density of DA at the 3D

gold electrode was greater by about 6 times than GC electrode and 12 times than gold disk electrode. The peak to peak separation (ΔE_p) value of DA at the three electrodes was also measured and resulting of 63 mV for 3D gold, 61 mV for gold disk, and 114mV for GC electrode. The small ΔE_p value indicates that fast electron transfer of DA occurred at both 3D gold and gold disk electrode surface. Figure 4B displays the combined differential pulse voltammograms of DA at the three electrodes. The peak potential of DA at the 3D gold and gold disk electrode were both seen at +0.13 V, whereas, at GC electrode the peak potential was observed at +0.15 V. The low peak potential and small ΔE_p value at the 3D gold and gold disk electrode shows that both electrodes possess superior electrocatalytic properties for DA oxidation. In addition, the high oxidation current density measured at the 3D gold electrode suggests improved sensitivity towards DA detection compared to GC and gold disk electrode. A scan rate study was conducted for the electrochemical oxidation and reduction of DA at the 3D gold electrode which confirmed a diffusion-controlled process (Figure S3 of Supporting Information).

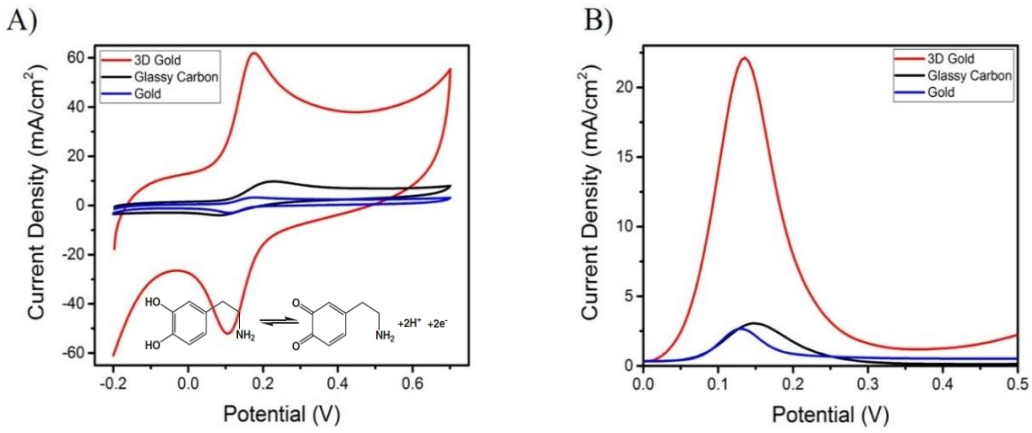

Figure 4. A) Cyclic voltammograms and B) Differential pulse voltammograms of 150 µM DA in 0.1 M phosphate buffer solution (pH 7.2) at the 3D gold, glassy carbon, and gold disk electrode.

Determination of Dopamine

CV and DPV were carried out for the quantification of DA in buffered solution. The concentration of DA was increasingly changed from 50 µM to 250 µM. Figure S4A-C shows the cyclic voltammograms conducted from -0.2 V to +0.7 V to observe both reduction and oxidation peak of DA with all three electrodes. The anodic and cathodic peak currents increased with

increasing concentration demonstrating good response for all electrodes. At the 3D gold electrode, the anodic peak shifted towards positive potential while the cathodic peak shifted towards more negative potential. At both GC and gold disk electrode, the oxidation and reduction peak potentials were similar as concentration increases. As DPV gives better sensitivity compared to CV, the technique was used to evaluate the linearity and the sensitivity for each electrodes for concentration of DA between 50 µM and 250 µM (Figure S4D-F). A clear oxidation signal with increased magnitude for increased DA concentration resulted for all electrodes and which was centered at around +0.12 V. Calibration plots are derived and combined in Figure 5. It can be seen that all electrodes presented excellent linearity with current density values proportionally increasing with DA concentration. Again, however different sensitivity could be noticed between the three electrodes. With the highest value of 0.07 mA cm^{-2} Mm^{-1} the 3D gold electrode showed the best performance and the highest sensitivity compared to GC and gold disk electrode which produced a calibration plot slope of 0.02 mA cm^{-2} Mm^{-1} and 0.015 mA cm^{-2} Mm^{-1}, respectively. The sensitivity of DA detection at the 3D gold is increased by 4.1 times compared to GC and 4.7 times compared to the commercial gold disk electrode.

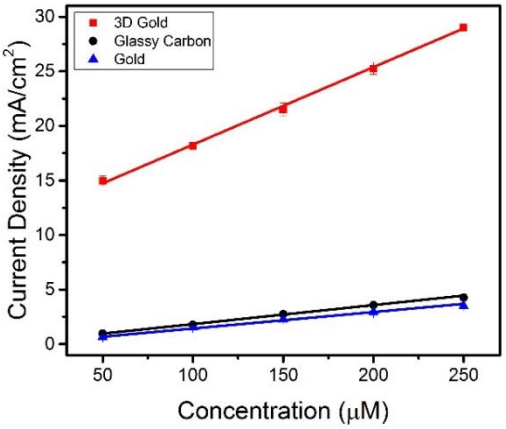

Figure 5. Calibration curve of the peak current density against the concentration of DA in the 0.1 M phosphate buffer solution (pH 7.2) at the 3D gold, glassy carbon, and gold disk electrode.

Simultaneous Detection of Acetaminophen and Dopamine

AC and DA could coexist in biological samples and thus the ability to selectively determine these two species is highly desired and thus, the electrochemical behavior of AC and DA in their mixture solution at the 3D gold, GC, and gold disk electrode was studied. CV was done to determine the anodic and cathodic peak of AC and DA in the mixture and the result is presented in Figure 6A. For the three electrodes, only the oxidations peaks of AC and DA were separated and clearly distinguishable. At the 3D gold electrode, the anodic peaks were observed at +0.16 V and +0.47 V for DA and AC, respectively. while the cathodic peak was observed at 0.10 V. Anodic peaks of DA and AC at +0.17 V and +0.40 V were recorded for the GC electrode, while the gold disk electrode produced anodic peaks at +0.16 V and +0.48 V for DA and AC, respectively. A better visualization can be obtained by using DPV analysis. Figure 6B shows the combined differential pulse voltammograms of AC and DA oxidation at the three electrodes. All three electrodes present very distinguishable signals for DA and AC with only little difference in the peak separation. The gold disk electrode gave better peak potential separation of about 317 mV, followed by 3D gold with value of 292 mV and GC with separation of 241 mV. The large separation of the anodic peak potentials allows better simultaneous detection of both analytes as the peaks are more distinguishable. Therefore, considering the better separation and the larger peak current density, the 3D gold electrode is used for the simultaneous detection of AC and DA. To demonstrate this ability, DPV measurements were carried out altering alternatively the concentration of both analytes (Figure 6C-D). Clearly the presence of either one analyte does not affect the quantification of the other, resulting a good performance for the detection of both DA and AC in a mixture similar to the one demonstrated for individual analysis. 3D gold electrode in fact presented sensitivity values of 0.06 mA cm^{-2} Mm^{-1} for DA and 33.80 mA cm^{-2} Mm^{-1} for AC, almost coincident with the values recorded for individual determination. Thus, considering the obtained result, the 3D gold electrode is feasible for the simultaneous detection of AC and DA in biological samples.

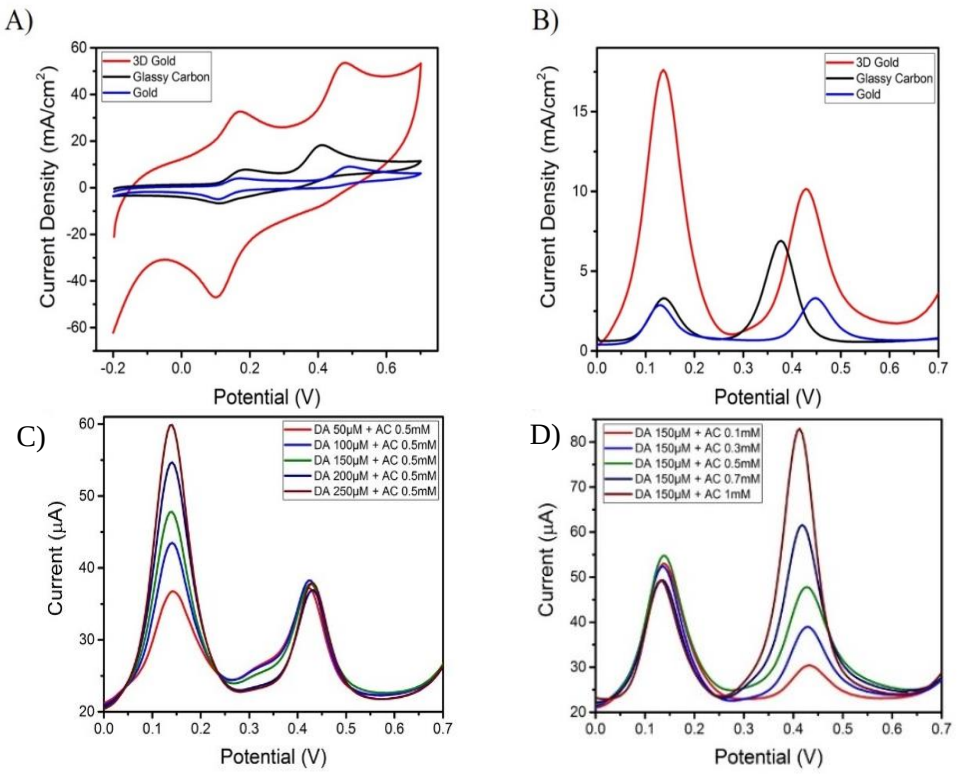

Figure 6. A) Cyclic voltammograms and B) Differential pulse voltammograms of 0.3 mM AC + 150 µM DA in 0.1 M phosphate buffer solution (pH 7.2) at the 3D Gold, glassy carbon, and gold disk electrode. Differential pulse voltammograms at 3D Gold electrode of C) 50 - 250 µM DA and 0.5 mM AC and D) 150 µM DA and 0.1 – 1 mM AC in 0.1M phosphate buffer solution (pH 7.2).

Determination of Acetaminophen in Pharmaceutical Tablets

To evaluate the feasibility of practical application at the 3D gold electrode in a real sample, quantification of AC in pharmaceutical commercial tablets were conducted. Using DPV technique and the AC individual calibration plot previously obtained, excellent correlation between real sample concentration and the one measured. Recovery test and performance results are summarized in Table 1.

Table 1 Recovery tests of acetaminophen in pharmaceutical tablets.

Sample	Content (μM)	Added (μM)	Found (μM)	Recovery (%)	R.S.D (%)
1	150	50	51.15	102.29	1.04
2	200	50	53.33	106.66	3.94
3	250	50	54.37	108.73	0.69

CONCLUSION

Here we evaluated the possibility of utilizing the 3D printing technology for the fabrication of electrochemical transducers for electroanalytical devices. In this study, the 3D-printed stainless steel electrode was electro-plated to deposit a thin gold film on the surface and employed as the working electrode. Cyclic voltammetry and differential pulse voltammetry techniques were employed for the individual and simultaneous detection of acetaminophen (AC) and dopamine (DA) in aqueous solutions. Through the investigation, the 3D gold electrode shows increased peak currents by enhanced electron transfer for both AC and DA at the electrode surface. The sensitivity of the 3D gold electrode was enhanced by about 3 times compared to that of GC and 4.7 times compared to that obtained with the commercial gold disk electrode for both individual and simultaneous detection. The proposed 3D-printed electrode was further utilized for determination of AC in pharmaceutical commercial tablets and satisfying recovery results were obtained. Therefore, the simple fabrication, high sensitivity, and good electro-catalytic property suggest that the gold-plated 3D-printed steel electrode is a promising candidate for practical use for electroanalytical applications.

ACKNOWLEDGMENTS

M.P. thanks Tier 1 (123/16) grant from ministry of Education, Singapore.

REFERENCES

1 Gebhardt, A. *Understanding additive manufacturing: rapid prototyping, rapid tooling, rapid manufacturing*; Hanser Publishers: Munich, 2012.

2 Nakamura, M.; Kobayashi, A.; Takagi, F.; Watanabe, A.; Hiruma, Y.; Ohuchi, K.; Iwasaki, Y.; Horie, M.; Morita, I.; Takatani, S. *Tissue Engineering* **2005**, *11* (11-12), 1658–1666.

3 Zhu, C.; Han, Y. J.; Duoss, E. B.; Golobic, A. M.; Kuntz, J. D.; Spadaccini, C. M.; Worsley, M. A., *Nat. Commun.* **2015**, *6*, 6962.

4 Horn, T. J.; Harrysson, O. L. A., *Sci. Prog.* **2002**, *95*, 255-282.

5 Mironov, V.; Visconti, R. P.; Kasyanov, V.; Forgacs, G.; Drake, C. J.; Markwald, R. R. *Biomaterials* **2009**, *30* (12), 2164–2174.

6 Duncan, J. M.; Daurka, J.; Akhtar, K., *Br. Med. J.* **2014**, 348.

7 Ambrosi, A.; Pumera, M. *Chem. Soc. Rev.* **2016**, *45*, 2740–2755.

8 Grieshaber, D.; MacKenzie, R.; Vörös, J.; Reimhult, E. *Sensors* **2008**, *8* (3), 1400 – 1458.

9 Ronkainen, N. J.; Halsall, H. B.; Heineman, W. R.*Chem. Soc. Rev.* **2010**, *39* (5), 1747 – 1763.

10 Loo, A. H.; Chua, C. K.; Pumera, M., *Analyst* **2017**, *142*, 279-283.

11 Adhikari, B.-R.; Govindhan, M.; Chen, A. *Electrochimica Acta* **2015**, *162*, 198–204.

12 Habibi, B.; Jahanbakhshi, M.; Pournaghi-Azar, M. H. *Electrochimica Acta* **2011**, *56* (7), 2888–2894.

13 Atta, N. F.; Galal, A.; Azab, S. M. *Intl. J. Electrochem. Sci.* **2011**, *6*, 5082-5096.

14 Babaei, A.; Dehdashti, A.; Afrasiabi, M. *Intl. J. Electrochem. Sci.* **2011**, *6*, xxx

15 Manikandan, P. N.; Dharuman, V. *Electroanalysis* **2017,** *29*, 1-9.

16 Zhang, Q.-L.; Feng, J.-X.; Wang, A.-J.; Wei, J.; Lv, Z.-Y.; Feng, J.-J. *Microchimica Acta* **2014**, *182* (3-4), 589–595.

17 Chen, Y.; Guo, L.-R.; Chen, W.; Yang, X.-J.; Jin, B.; Zheng, L.-M.; Xia, X. H. *Bioelectrochemistry* **2009**, *75* (1), 26–31.

18 Raj, C. R.; Ohsaka, T. *J. Electroanal. Chem.* **2001**, *496* (1-2), 44–49.

19 Raj, C.; Okajima, T.; Ohsaka, T. *J. Electroanal. Chem* **2003**, *543* (2), 127–133.

20 Ambrosi, A.; Moo, J. G. S.; Pumera, M. *Adv. Funct. Mater.* **2016**, *26*, 698.

21 Fischer, L. M.; Tenje, M.; Heiskanen, A. R.; Masuda, N.; Castillo, J.; Bentien, A.; Émneus, J.; Jakobsen, M. H.; Boisen, A. *Microelectronic Engineering* **2009**, *86* (4-6), 1282–1285.